Title

Structural and functional correlates of olfactory reward processing in behavioral variant frontotemporal dementia.

Authors

Sokołowski, Andrzej
Brown, Jesse
Roy, Ashlin
et al.

Publication Date

2024-12-01

DOI

10.1016/j.cortex.2024.09.011

Peer reviewed

HHS Public Access

Author manuscript

Cortex. Author manuscript; available in PMC 2025 February 10.

Published in final edited form as:

Cortex. 2024 December ; 181: 47–58. doi:10.1016/j.cortex.2024.09.011.

Structural and functional correlates of olfactory reward processing in behavioral variant frontotemporal dementia

Andrzej Sokołowski[1], **Jesse A. Brown**[1], **Ashlin R.K. Roy**[1], **Noah Cryns**[1], **Aaron Scheffler**[2], **Emily G. Hardy**[1], **Samir Datta**[1], **William W. Seeley**[1,3], **Virginia E. Sturm**[1], **Bruce L. Miller**[1], **Howard J. Rosen**[1], **David C. Perry**[1]

[1]Department of Neurology, Memory and Aging Center, UCSF Weill Institute for Neurosciences, University of California San Francisco, San Francisco, CA 94158, USA

[2]Department of Epidemiology and Biostatistics, University of California San Francisco, San Francisco, CA, 94158, USA

[3]Department of Pathology, University of California San Francisco, San Francisco, CA 94158, USA

Abstract

The behavioral variant of frontotemporal dementia (bvFTD) includes symptoms that reflect altered pursuit of rewards, including food, alcohol, and money. Little is known, however, about how these reward changes relate to atrophy and functional connectivity within reward-related regions. The goal of this study was to examine the structural and functional correlates of valence perception for olfactory rewards in 24 patients with bvFTD. Regression analysis of resting-state brain functional connectivity indicated that more positive valence ratings of olfactory stimuli were predicted by ventral pallidum connectivity to other reward circuit regions, particularly functional connectivity between ventral pallidum and bilateral anterior cingulate cortex/ventromedial prefrontal cortex. Structural analysis showed that atrophy of the anterior cingulate cortex was also significantly associated with perceiving stimuli as more rewarding. Finally, there was a significant interaction between ventral pallidum connectivity and atrophy of the anterior cingulate cortex. More specifically, the ventral pallidum connectivity had a greater effect on the positive perception of olfactory stimuli in the setting of low anterior cingulate cortex volume. These findings indicate that atrophy and functional connectivity within reward-relevant regions exert independent and interacting effects on the perception of pleasantness in bvFTD, potentially due to changes in hedonic “liking” signals.

Keywords

reward; dementia; bvFTD; functional connectivity

Correspondence to: David C. Perry, University of California, San Francisco (UCSF), Memory and Aging Center, Box 1207, 675 Nelson Rising Lane, Suite 190, San Francisco, CA 94143, David.Perry@ucsf.edu.

1. Introduction

Reward processing drives goal-directed behavior and is an important element underlying adaptive responses to environmental stimuli (Haber & Knutson, 2010). The definition of what constitutes a reward is broad, encompassing stimuli that pertain to approach or avoidance, consumption, learning based on feedback, and hedonic feelings (Schultz, 2010). The absence of reward or the experience of aversive stimuli constitutes punishment (Lutz & Widmer, 2014), which may exist on the same spectrum as reward or may have distinct features in their processing.

Many symptoms and behaviors in the behavioral variant of frontotemporal dementia (bvFTD) are secondary to alterations in reward processing. Apathy, euphoria, and disinhibition are complex constructs in which a change in perception of reward or punishment may play a contributing role. Individuals with bvFTD often overeat and prefer food high in sucrose. Overeating may be explained by altered sensory processing, persistence of the rewarding value of food despite consumption, or a decreased sensitivity to aversive feedback (Perry & Kramer, 2015). Some patients with bvFTD exhibit hypersexuality, hyposexuality, or inappropriate sexual behavior (Ahmed et al., 2015; Miller et al., 1995; Perry et al., 2014). Shifts in the perception of specific types of reward occur in bvFTD, including greater willingness to expend effort to obtain monetary compared to social reward (Perry et al., 2015). Most people with bvFTD make risky monetary decisions within laboratory paradigms (Torralva et al., 2007), which may explain the high prevalence of real-life financial errors with this condition (Chiong et al., 2014). Also, they favor immediate rewards, impulsively discounting the value of rewards that involve delay (Bertoux et al., 2015).

Numerous brain regions modulate reward processing. Animal and human studies identify a complex brain network involved in reward (Haber & Knutson, 2010). One of the main structures involved in reward processing is the nucleus accumbens, which is part of the ventral striatum (VS; Bartra et al., 2013; Daniel & Pollmann, 2014). VS receives dopaminergic projections from ventral tegmental area (VTA), as well as input from orbitofrontal cortex (OFC)/ventromedial prefrontal cortex (vmPFC), and projects to ventral pallidum (VP), which projects to the dorsomedial nucleus of the thalamus (Haber & Knutson, 2010), then back to cortex. VP is connected to many other regions and receives glutamatergic input from medial prefrontal cortex, subthalamic nucleus, thalamus, amygdala, and habenula as well as cholinergic inputs from nucleus accumbens, amygdala, VTA, and prefrontal cortex (Kupchik & Prasad, 2021; Root et al., 2015). Some human studies reveal that dopaminergic activity in both VS and VP plays a role in reward processing (Cohen et al., 2009; Pribiag et al., 2021; Zaehle et al., 2013). Of importance, there is a link between VS dopamine release and fMRI signal (Knutson & Gibbs, 2007). Anterior cingulate cortex (ACC), especially its dorsal region, integrates affective and cognitive information and resolves reward-related conflicts (Bush et al., 2000; Silvetti et al., 2014). Specific regions within the reward circuit have differing roles depending on the type or aspect of reward. Kringelbach and Rolls (2004) find that medial OFC is responsible for monitoring reward value and lateral OFC for evaluation of punishment. The vmPFC plays a role in reward consumption and processes reward magnitude (Diekhof et al., 2012).

Regions that degenerate in early bvFTD overlap with reward processing regions (Perry & Kramer 2015) and correlate with behaviors that underly shifts in reward processing. Overeating and sucrose preference correlate with atrophy in OFC, insula, striatum, ventral putamen, and pallidum (Ahmed et al., 2016; Whitwell et al., 2007; Woolley et al., 2007). Previously, we explored the structural correlates of increased pursuit of primary rewards, including food, drugs, and sex (Perry et al, 2014) and found that increased reward-seeking behavior was associated with atrophy in the right ventral putamen and pallidum.

While many previous studies explored the relationship between focal atrophy and behavior, the regions studied do not work in isolation during reward processing. Rather, they work as a functional circuit (Belin & Everitt, 2008; Haber et al., 2006). In addition to structural changes, bvFTD has also been associated with functional connectivity changes involving reward regions, as many of these structures form parts of large-scale networks that degenerate in FTD, including the salience and semantic appraisal networks (Ranasinghe et al., 2016; Zhou et al., 2010).

The functional correlates of reward processing in bvFTD are as yet unknown. Using a laboratory task that employs olfactory stimuli, previously we identified changes in perception of pleasant and unpleasant smell in bvFTD, suggesting that differences in the perception of valence is an important factor underlying changes in motivated behavior (Perry et al., 2017). Blunted sensitivity to unpleasant stimuli or decreased distinction between positive and negative valence were associated with degeneration in structures involved in reward, including insula and amygdala; however, the functional correlates of the perception of pleasant and unpleasant stimuli in bvFTD have not been identified, and it is unknown whether altered perception of valence is best explained by structural or functional connectivity changes. Using the previously described olfactory reward task (Perry et al, 2017), the goal of this study was to examine neural correlates of specific components of reward processing in patients with bvFTD using resting-state functional connectivity of brain regions that have either been previously linked to reward-related behavior changes in bvFTD or found to have a role in reward processing more broadly. While our prior findings suggest volume of structures including amygdala and insula may relate to perception of negative stimuli or ability to distinguish positive from negative stimuli, we hypothesized that functional connectivity of structures previously linked to primary reward and pleasantness, namely ventral putamen and pallidum, would be associated with overall valence perception of olfactory stimuli (Perry et al., 2014).

2. Material and methods

2.1. Participants

Twenty-four participants (9 female), aged 49 – 76 (M = 63.20; SD = 6.89), were recruited and evaluated at the University of California San Francisco (UCSF) Memory and Aging Center. All were given a bvFTD clinical diagnosis, met International bvFTD Criteria Consortium criteria for at least possible bvFTD (Rascovsky et al., 2011), underwent structural and functional resting-state (eyes closed) MRI scans, and performed an odor reward task (Perry et al., 2017). All assessments were conducted within 6 months (M = 1.3 days; SD = 3.21) from MRI scans. Additionally, the Clinical Dementia Rating scale

sum-of-boxes (CDR-SB; Morris 1993) was used to measure the severity of global functional impairment. Written informed consent was obtained from patients or surrogates according to procedures approved by the UCSF Committee on Human Research. We report how we determined our sample size, all data exclusions, all inclusion/exclusion criteria, whether inclusion/exclusion criteria were established prior to data analysis, all manipulations, and all measures in the study. No part of the study procedures or analysis plans was preregistered prior to the research being conducted. Public archiving of the anonymized data is not permitted under the study's IRB approval due to the sensitive nature of patient data; however, data are available upon request by submitting a UCSF MAC Resource Request form: http://memory.ucsf.edu/resources/data. Following a UCSF-regulated procedure, access will be granted in line with ethical guidelines on the reuse of sensitive data, including submission of a Material Transfer Agreement, available at: https://icd.ucsf.edu/material-transfer-and-data-agreements. Analysis codes, scripts, and digital study materials are available on the publicly accessible digital repository 'Open Science Framework' (OSF; https://osf.io/e7u2f/).

2.2. Odor reward task

Participants performed a reward consumption task involving the sequential presentation of a series of seven olfactants in glass vials. Pleasant, or positive valence olfactants included vanillin (8% in propylene glycol), menthol (10% in propylene glycol), and citral (10% in propylene glycol). Unpleasant, or negative valence olfactants included isovaleric acid (5% in propylene glycol), propionic acid (1% in propylene glycol), and pyridine (1% in propylene glycol). Propylene glycol (100%) was used as a neutral stimulus. Olfactants were obtained from Sigma-Aldrich. The stimuli were used in previous studies and have consistently been rated as having the desired positive or negative valence (Bensafi et al., 2002; Rolls et al., 2003; Perry et al., 2017).

Tasks were administered in E-prime (11 patients with version 2.0; 13 patients with version 3.0; Psychology Software Tools, Pittsburgh, PA). Upon a cue participants inhaled, exhaled, and then sniffed for 3 s while the experimenter placed a glass vial beneath their nose. Stimuli were presented in random order and subjects were asked to rate the pleasantness of each smell on a 1–9 scale with 1 indicating very unpleasant, 9 representing extremely pleasant, and 5 being neutral. Each stimulus was presented once. Trial duration varied between 46 and 88 seconds, with an interstimulus interval used to allow olfactants to dissipate and prevent olfactory habituation, plus a variable amount of time for participants to answer questions. Valence scores were calculated as the means of the three pleasant and three unpleasant stimuli and for the six stimuli together. To ensure that the results were not impacted by olfactory acuity, sixteen participants completed an odor discrimination task. We presented each participant with ten pairs of smells (using the same olfactants) and asked them if these two smells were the same or different from each other. We calculated a discrimination score based on accuracy of responses and correlated this score with valence ratings.

2.3. Image acquisition

Structural and resting-state functional scans were acquired at the UCSF Neuroscience Imaging Center using a 3T Siemens Prisma Fit MRI scanner. Whole-brain T1-weighted images were acquired with sagittal slice orientation using the following parameters: 1 × 1

× 1 mm resolution; slices per slab = 160; matrix = 240 × 256; repetition time = 2.3 ms; inversion time = 900 ms; flip angle = 9°; echo time = 2.9 ms. Functional images were acquired using two sets of parameters: 15 subjects were scanned in transversal orientation; acquisition time = 10 min; repetition time = 3000 ms; echo time = 30 ms; 3.3 × 3.3 × 3.3 mm resolution; 50 slices; 197 volumes. Nine subjects were scanned in transversal orientation; acquisition time = 8:05 min; repetition time = 850 ms; echo time = 32.8 ms; 2.2 × 2.2 × 2.2 mm resolution; 66 slices; 560 volumes.

2.4. Image preprocessing

Images were preprocessed using fMRIPrep (Esteban et al., 2019). Functional images were co-registered to the T1-weighted reference using FSL's flirt and slice-time corrected with AFNI's 3dTshift, resampled into MNI standard space with ANTs, and spatially smoothed with an isotropic Gaussian 6 mm kernel. Segmentation of CSF, white matter, and gray matter was performed with FSL's fast. Voxel-wise timeseries were temporally bandpass filtered with 128s cut-off; global signal, mean tissue signals, and Friston 24 head motion parameters (six rotational and translational parameters, squares, and temporal derivatives) were regressed out. All data had mean framewise displacement score below 0.55 ($M = 0.13$; $SD = 0.12$) with all frames below the threshold.

Gray matter volume (GMV) was calculated by voxel-based morphometry (VBM) using CAT12 (v. 12.7; r1742; Gaser et al., 2024). T1-weighted images were normalized to MNI space and segmented into gray matter, white matter, and cerebrospinal fluid. GMV of each region of interest (ROI) was extracted and divided by total intracranial volume for each subject.

2.5. Reward network

Based on prior literature (see Haber & Knutson, 2010 for a review) we selected 15 bilateral ROIs that are involved in reward processing. Bilateral pregenual ACC, amygdala, dorsal caudate, dorsolateral putamen, nucleus accumbens, insula (ventral agranular, ventral granular, dorsal), and orbital gyrus (lateral, medial anterior, and medial posterior) were taken from the Brainnetome atlas (Fan et al., 2016). Bilateral thalamus was taken from the Automated Anatomical Labelling atlas 3 (Rolls et al., 2020). Habenula, VTA, and VP ROIs were taken from CIT168 atlas (Pauli et al., 2018). Multiple atlases were used to ensure the best spatial localization of the regions. ROIs are pictured (Figure S1) in the supplementary material.

2.6. Connectivity analyses

Node-to-network functional connectivity was calculated for each ROI separately. Functional connectivity is defined as a correlation between timeseries. Node-to-network connectivity, also called within-network weighted degree, represents the sum of correlations between a given ROI and all the other voxels within a reward network mask comprised of the ROIs listed above. Node-to-network connectivity represents a strength of the relationship between a given node and the rest of the reward network associated with the particular process in question or presence of the disease (Hayasaka & Laurienti, 2010; Rubinov & Sporns, 2010). Seed-based functional connectivity analysis was performed using ROIs that significantly

predicted valence (variable selection is described in the statistical analyses section). SPM12 was used to run the analyses.

2.7. Statistical analyses

As a first step, node-to-network functional connectivity scores and GMV were harmonized across the two scanners with ComBat (Fortin et al., 2016). ComBat uses a robust algorithm to remove scan variability introduced by different scanners and corrects for inter-subject differences that may occur in result of using different scanners (Redua et al., 2020; Torbati et al., 2021) or different acquisition protocols (Dole et al., 2023). This approach has been used in MRI studies with dementia patients (Thomopoulos et al., 2021; Zhang et al., 2023). We provide an example of a native-space image (Figure S2) as well as averaged normalized images (Figure S3) for the data from the two scanners in the supplementary material.

To test the relationship between the functional data and reward processing, the node-to-network functional connectivity scores from all bilateral ROIs were entered into a single regression model as predictors of mean valence scores. To ensure that there was no lateralization effect significant bilateral ROIs were subsequently tested separately for the right and left regions using correlation models with valence. Furthermore, our prior study showed differences in the perception of unpleasant vs. pleasant valence in bvFTD (Perry et al., 2017). Therefore, to ensure that functional connectivity relationships did not differ between olfactants with positive or negative valence, correlations for mean valence ratings of pleasant and unpleasant stimuli were tested separately as well. Regression models were run using the ncvreg (3.13) package in R. Minimax concave penalty (MCP; Zhang 2010) penalized regression models were used to prevent overfitting and deal with a larger number of predictors. MCP regression is a type of variable selection method that uses penalized regression with a regularization term lambda. Leave-one-out cross-validation was used to calculate the value of lambda. Marginal false discovery rate (mFDR) was used for feature selection (Breheny, 2019). Models were corrected for age and sex.

After identifying regions whose connectivity to the entire network predicted valence ratings, we used seed-based voxel-wise connectivity analyses for significant ROIs to determine the connectivity relationships within the reward network that are most strongly associated with perception of valence.

While our primary objective was to identify the functional correlates of valence perception, we performed additional analyses to determine the role of structural changes, either alone or along with functional ones. First, to identify the effect of volumetric changes, VBM analysis was used to test if structural atrophy in the same 15 ROIs related to overall valence. Next, to answer the question of whether there are effects of both atrophy and functional connectivity on reward processing, GMV of all ROIs and functional connectivity scores for significant ROIs were entered to a regression model using the ncvreg package in R. Finally, a general linear regression model with an interaction between functional connectivity and GMV was used to test whether there is an interaction between significant functional and structural findings. Models were corrected for age and sex.

3. Results

Twenty-four patients with bvFTD completed the odor reward task. Their mean CDR-SB was 5.98 (SD = 2.6). Their mean valence rating for the six stimuli was 5.25 (SD = 1.47) (valence rating of negative stimuli M = 4.82; SD = 1.73; valence rating of positive stimuli M = 5.68; SD = 1.42). The mean olfactory discrimination score was 73%. The correlation of discrimination scores with overall valence scores was non-significant (p = .64), suggesting that loss of olfactory acuity was not driving perception of valence.

A regression model was used to determine the node-to-network functional connectivity predictors of mean valence ratings. The only significant predictor was bilateral VP connectivity (est. = .404, z = 3.07, mFDR = .0283 at lambda .261) with higher VP connectivity predicting more positive valence. There was no relationship between valence and CDR-SB (r = − .05; p = .81), therefore CDR-SB was not used as a covariate in the analyses.

To test whether the effect of VP connectivity differed based on lateralization, we separately assessed the correlations between right or left VP connectivity and valence ratings (Figure 1). Valence significantly correlated with connectivity of both left (r = .56; p = .004) and right VP (r = .43; p = .03), indicating no lateralization effect. To test whether VP connectivity had differing effects on the rating of pleasant or unpleasant stimuli, we tested correlations for each separately. Bilateral VP connectivity positively correlated with valence ratings of both pleasant (r = .43; p = .04) and unpleasant olfactory stimuli (r = .57; p = .004), suggesting an overall effect on ratings across the spectrum of valence.

To investigate the degree of scanner effect on these results both before and after harmonization we conducted a series of tests. First, we visualized the edge weights using t-distributed Stochastic Neighbor Embedding (t-SNE) before and after harmonization. This scatter-plot visualization allows us to assess the distribution and variation of edge weights to help understand how much of the variation can be attributed to differences between scanners. We found that data were not strongly segregated initially and were more intermixed after harmonization (Figure S4). To further investigate whether harmonization removed scan variability, we performed Kruskal-Wallis tests to determine if there was a difference in all 378 connectivity edges between the two scanners. No pairs were significantly different between the two scanners, either before or after harmonization. FDR-corrected p-values post harmonization were close to 1 showing no significant effect of scanner (Figure S5). We then selectively inspected the distribution of connectivity edges of key importance to our central finding (VP – ACC) and found little difference between the two scanners after harmonization (Figure S6). In order to assess for a possible effect of scanner on the reported findings, we calculated correlation coefficients for VP connectivity to valence ratings separately for each of the two scanners. Valence significantly correlated with bilateral VP connectivity in the scanner 1 (n = 15; r = .47; p = .02) and not in the smaller group tested on scanner 2 (n = 9; r = .47; p = .2); however, the difference between the two correlation coefficients tested with Fisher's z-transformation was not significant (z = .14; p = .68). This series of analyses indicates that for the functional connections between the 28 ROIs there was no significant difference between the two scan protocols,

with minimal scanner effects before harmonization, and reduction of scanner effect achieved by the use of ComBat.

Voxel-wise functional connectivity analysis was performed with the bilateral VP as a seed to determine for which regions VP connectivity best predicts valence. The analysis was masked to the reward network. The analysis yielded one significant cluster encompassing portions of bilateral ACC/vmPFC (Figure 2, k = 689; peak MNI [−6 36 −8]; peak t = 8.01; FWE < .05) with higher connectivity predicting more positive valence.

VBM analysis was performed to test if volume of any brain region within the reward network was a predictor of valence. No cluster survived FWE correction; however, the volume of an dorsal ACC cluster (k = 30; Brodmann area 32) was a negative predictor of valence at the uncorrected level (Figure 3, p < .001; FWE > .05) with smaller volume predicting more positive valence.

To determine whether functional connectivity results remain significant after controlling for GMV a regression model with node-to-network bilateral VP functional connectivity and GMV of all reward network ROIs was used. VP functional connectivity remained a significant predictor (est. .57, z = 4.3; mFDR < .001). Additionally, the GMV of pregenual ACC was a significant negative predictor of valence (est. − .55; z = −4.2, mFDR = .001) at lambda .184.

Finally, to determine whether there is an effect modification of functional connectivity and volume, a general linear regression model was run with VP functional connectivity, pregenual ACC ROI volume, and their interaction as predictors of valence. VP functional connectivity was a significant positive predictor ($t = 3.02$; $p < .01$), pregenual ACC volume was a negative predictor of valence ($t = -2.72$; $p < .05$), and their interaction was significant ($t = -2.17$; $p < .05$); F = 8.18, $p < .001$. An interaction plot with pregenual ACC volume split into high and low groups (Figure 4) indicated that the effect of VP connectivity on valence ratings is greater in the setting of low pregenual ACC volume.

4. Discussion

While abnormal reward-related behaviors in bvFTD have previously been associated with volumetric changes, there is little evidence regarding how reward perception relates to changes in functional connectivity. Here, by relating resting state functional connectivity to performance on an olfactory reward task, we found that greater VP connectivity to other reward-relevant structures is associated with more positive perception of valence in bvFTD. The association between VP connectivity and valence particularly relates to both the structure and connectivity of the ACC. Valence ratings positively correlate with the strength of the VP to ACC connection, and while low ACC volume itself predicts higher valence ratings, there is also a significant interaction, indicating that VP connectivity has a stronger positive correlation with valence ratings when ACC volume is low.

Identification of the VP as a key area in the perception of valence is consistent with prior evidence regarding its structure and function. The VP has extensive and complex structural reward circuit connections, not only with VS, but also to the thalamus, VTA/

dopaminergic midbrain, habenula, subthalamic nucleus, hypothalamus, dorsal pallidum, and pedunculopontine nucleus (Haber & Knutson, 2010). VP adjoins the olfactory tubercle, making this region relevant for processing the type of olfactory reward used in this task (Xiong & Wesson, 2016), however, the VP has a broader role across reward modalities. Reward processing can be divided into two components: hedonic "liking" and "wanting" due to incentive salience (Berridge et al., 2009). VP is a crucial element in the processing of rewards and regulates hedonic "liking" reactions (Smith & Berridge, 2005). The valence ratings in this olfactory task focus on this "liking" component of rewarding stimuli. Hedonic "liking" underlies subjective pleasure associated with reward, but also relates to physiological reactions to it and objective changes in behavior (Berridge et al., 2009). Individuals have stronger activity of this part of the reward network when they perceive stimuli as more rewarding. Alternatively, higher activity of the VP may also lead to the perception of stimuli as more rewarding. Its neurons code hedonic impact of stimuli and stay active even after shifting the hedonic value of rewards, which may result in positive reactions to stimuli that were not previously perceived as pleasant (Smith & Berridge, 2005).

This finding linking VP connectivity to increased "liking" has implications for the range of reward phenotypes that exist in bvFTD. Symptoms in bvFTD reveal multiple potential reward changes (Sturm et al., 2015). Typically, there is apathy, or blunted motivation to act to rewards, but also increased pursuit of certain rewards, such as food, sex, and alcohol (Perry et al., 2014). There may be different reasons for these varied reward changes, with distinct neuroanatomic correlates. For example, we find that right-lateralized, largely subcortical volume loss is associated with increased primary reward seeking (Perry et al., 2014). Also, we identified partially overlapping reward circuit structural changes associated with perceiving negative stimuli as more pleasant and blunted differentiation between positive and negatively valenced stimuli (Perry et al., 2017). In the current study we see the imaging correlates of a different phenotype, which is greater valence perception across both positive and negative stimuli. Continued pursuit of rewarding stimuli, such as sweet food, in the absence of motivational salience could be linked to blunting of the salience update associated with "wanting" but could also relate to ongoing high "liking" signal from VP (Tindell et al., 2006).

The complex relationship we found between valence ratings, VP to ACC connectivity, pregenual ACC volume, and the interaction between VP to ACC connectivity and pregenual ACC volume could clarify the role of these structures in the reward changes observed in bvFTD. Patients with bvFTD showed higher valence ratings with greater connectivity between VP and ACC/vmPFC. These regions are part of a larger striato-pallido-cortical circuit. The VP is structurally linked with the ACC via VS projections (Haber & Knutson, 2010; Ikemoto, 2007), then projects back to ACC via the thalamus. Smith et al. (2009) suggested that VP, with its connections to ACC and other vmPFC regions, is a final common pathway for reward processing. There is evidence that VP and ACC are functionally linked as well, with a prior study showing hedonic modulation of ACC activity by the VP (van Steenbergen et al., 2015). Structures encompassing the reward network (ACC in particular) have been found to also be part of other, established large-scale brain networks, particularly the ventral salience network (Touroutoglou et al., 2012). This overlap provides an additional

model for interpreting our results and supporting rationales for why connectivity or volume of these regions may relate to the perception of valence.

Volume of the ACC was an independent negative predictor of valence ratings. ACC integrates reward, emotion, action feedback, and autonomic information (Rolls, 2019) and is a hub in the salience network, which undergoes targeted degeneration and dysfunction in bvFTD (Perry et al., 2017; Zhou et al., 2010). While ACC atrophy in FTD has often been associated with apathy, or lower motivation to pursue reward (Zamboni et al., 2008), a recent paper identified lower ACC volume as part of a "gating factor" for a range of reward-related changes in dementia (Chokesuwattanaskul et al., 2023). Alternatively, the effect of ACC atrophy on valence could relate to blunting of negative information, leading to more positive perception. Among patients with neurodegenerative disease, lower ACC volume is associated with lower sensitivity to punishment or behavioral inhibition (Shinagawa et al., 2015). The observation that valence relates to both decreased volume and increased connectivity in this same structure could relate to differing effects of distinct regions within the ACC. The dorsal portion may be more involved in appraisal or expression of negative affect or pain (Etkin et al., 2011; Shackman et al., 2011). Others have found that dorsal and rostral portions of ACC reciprocally suppress each other's activity (Bush et al., 2000). Both findings suggest that atrophy in a more dorsal portion of ACC (including the location of the cluster peak associated with valence in Figure 3) could remove suppression of the rostral, pregenual area shown in Figure 2, allowing for greater expression of the hedonic input from VP. This model could account for the observed interaction, in which the effect of VP connectivity on valence ratings was greater in the setting of low ACC volume, although since the ACC is an important hub for emotional processing and is interconnected with other brain regions (Bush et al., 2000), it can be expected that its atrophy will also impact the integration and functioning of other large-scale brain networks (Sporns, 2022).

One study limitation is that the task employed olfactory stimuli to target the reward system. As in a prior study (Perry et al., 2017), we did not find a correlation between valence ratings and odor discrimination, suggesting that olfactory acuity is unlikely to influence findings. People with bvFTD had impaired odor identification but not discrimination in prior studies (Silva et al., 2019). It is unclear to what extent the results of this study generalize to other reward types, including secondary rewards (e.g., monetary reward). The focus of this study was to examine regions most consistently identified as belonging to a reward network, and our results do not preclude the likely possibility that other brain regions are involved in reward processing. For example, frontal regions such as frontal pole, which we previously found to be associated with perception of negative stimuli (Perry et al., 2017), could be pertinent to reward perception in spite of being less consistently identified in reward studies, suggesting the need for broader future studies. Furthermore, we did not include an assessment of "wanting" component of rewards. Hence, future research will be needed to determine the specificity of our finding for valence. Our study is also limited by a relatively small sample size.

Clarifying the mechanistic underpinnings of reward-related behaviors in degenerative brain illness can help refine diagnosis and inform potential symptomatic treatment strategies; however, identifying plausible interventions may require knowledge beyond structural

volumetric changes alone. In this study, we expand upon previous studies relating reward changes to atrophy by demonstrating how the interrelationship between VP and ACC connectivity and structure influences valence perception in bvFTD. Further studies can help uncover how intervention targeting these connections and large-scale networks could counteract the debilitating symptoms associated with abnormal reward and motivation.

Supplementary Material

Refer to Web version on PubMed Central for supplementary material.

Funding

This study was supported by grants P01AG019724 (BLM), P30AG062422 (BLM), R01AG019724 (DCP), and R01AG062758 (DCP) from the National Institutes of Health.

References

Ahmed RM, Kaizik C, Irish M, Mioshi E, Dermody N, Kiernan MC, & Hodges JR (2015). Characterizing sexual behavior in frontotemporal dementia. Journal of Alzheimer's Disease, 46(3), 677–686. 10.3233/JAD-150034

Ahmed RM, Irish M, Henning E, Dermody N, Bartley L, Kiernan MC, & Hodges JR (2016). Assessment of eating behavior disturbance and associated neural networks in frontotemporal dementia. JAMA neurology, 73(3), 282–290. 10.1001/jamaneurol.2015.4478 [PubMed: 26810632]

Bartra O, McGuire JT, & Kable JW (2013). The valuation system: a coordinate-based meta-analysis of BOLD fMRI experiments examining neural correlates of subjective value. Neuroimage, 76, 412–427. 10.1016/j.neuroimage.2013.02.063 [PubMed: 23507394]

Belin D, & Everitt BJ (2008). Cocaine seeking habits depend upon dopamine-dependent serial connectivity linking the ventral with the dorsal striatum. Neuron, 57(3), 432–441. 10.1016/j.neuron.2007.12.019 [PubMed: 18255035]

Bensafi M, Rouby C, Farget V, Bertrand B, Vigouroux M, & Holley A (2002). Autonomic nervous system responses to odours: the role of pleasantness and arousal. Chemical senses, 27(8), 703–709. 10.1093/chemse/27.8.703 [PubMed: 12379594]

Berridge KC, Robinson TE, & Aldridge JW (2009). Dissecting components of reward:'liking', 'wanting', and learning. Current opinion in pharmacology, 9(1), 65–73. 10.1016/j.coph.2008.12.014 [PubMed: 19162544]

Bertoux M, de Souza LC, Zamith P, Dubois B, & Bourgeois-Gironde S (2015). Discounting of future rewards in behavioural variant frontotemporal dementia and Alzheimer's disease. Neuropsychology, 29(6), 933. 10.1037/neu0000197 [PubMed: 25893971]

Breheny PJ (2019). Marginal false discovery rates for penalized regression models. Biostatistics, 20(2), 299–314. 10.1093/biostatistics/kxy004 [PubMed: 29420686]

Bush G, Luu P, & Posner MI (2000). Cognitive and emotional influences in anterior cingulate cortex. Trends in cognitive sciences, 4(6), 215–222. 10.1016/S1364-6613(00)01483-2 [PubMed: 10827444]

Chiong W, Hsu M, Wudka D, Miller BL, & Rosen HJ (2014). Financial errors in dementia: testing a neuroeconomic conceptual framework. Neurocase, 20(4), 389–396. 10.1080/13554794.2013.770886 [PubMed: 23550884]

Cohen MX, Axmacher N, Lenartz D, Elger CE, Sturm V, & Schlaepfer TE (2009). Neuroelectric signatures of reward learning and decision-making in the human nucleus accumbens. Neuropsychopharmacology, 34(7), 1649–1658. 10.1038/npp.2008.222 [PubMed: 19092783]

Chokesuwattanaskul A, Jiang H, Bond RL, Jimenez DA, Russell LL, Sivasathiaseelan H, & Warren JD (2023). The architecture of abnormal reward behaviour in dementia: Multimodal hedonic phenotypes and brain substrate. Brain Communications, 5(2), fcad027. 10.1093/braincomms/fcad027 [PubMed: 36942157]

Daniel R, & Pollmann S (2014). A universal role of the ventral striatum in reward-based learning: evidence from human studies. Neurobiology of learning and memory, 114, 90–100. 10.1016/j.nlm.2014.05.002 [PubMed: 24825620]

Diekhof EK, Kaps L, Falkai P, & Gruber O (2012). The role of the human ventral striatum and the medial orbitofrontal cortex in the representation of reward magnitude–An activation likelihood estimation meta-analysis of neuroimaging studies of passive reward expectancy and outcome processing. Neuropsychologia, 50(7), 1252–1266. 10.1016/j.neuropsychologia.2012.02.007 [PubMed: 22366111]

Dole L, Schilling KG, Kang H, Gore JC, & Landman BA (2023). Harmonization of repetition time and scanner effects on estimates of brain hemodynamic response function. Proceedings of SPIE--the International Society for Optical Engineering, 12464, 124640X. 10.1117/12.2653903

Esteban O, Markiewicz CJ, Blair RW, Moodie CA, Isik AI, Erramuzpe A, & Gorgolewski KJ (2019). fMRIPrep: a robust preprocessing pipeline for functional MRI. Nature methods, 16(1), 111–116. 10.1038/s41592-018-0235-4 [PubMed: 30532080]

Etkin A, Egner T, & Kalisch R (2011). Emotional processing in anterior cingulate and medial prefrontal cortex. Trends in cognitive sciences, 15(2), 85–93. 10.1016/j.tics.2010.11.004 [PubMed: 21167765]

Fan L, Li H, Zhuo J, Zhang Y, Wang J, Chen L, & Jiang T (2016). The human brainnetome atlas: a new brain atlas based on connectional architecture. Cerebral cortex, 26(8), 3508–3526. 10.1093/cercor/bhw157 [PubMed: 27230218]

Fortin JP, Sweeney EM, Muschelli J, Crainiceanu CM, Shinohara RT, & Alzheimer's Disease Neuroimaging Initiative. (2016). Removing inter-subject technical variability in magnetic resonance imaging studies. NeuroImage, 132, 198–212. 10.1016/j.neuroimage.2016.02.036 [PubMed: 26923370]

Gaser C, Dahnke R, Thompson PM, Kurth F, Luders E, & Alzheimer's Disease Neuroimaging Initiative. (2024). CAT: a computational anatomy toolbox for the analysis of structural MRI data. GigaScience, 13, giae049. 10.1093/gigascience/giae049 [PubMed: 39102518]

Haber SN, Kim KS, Mailly P, & Calzavara R (2006). Reward-related cortical inputs define a large striatal region in primates that interface with associative cortical connections, providing a substrate for incentive-based learning. Journal of Neuroscience, 26(32), 8368–8376. 10.1523/JNEUROSCI.0271-06.2006 [PubMed: 16899732]

Haber SN, & Knutson B (2010). The reward circuit: linking primate anatomy and human imaging. Neuropsychopharmacology, 35(1), 4–26. 10.1038/npp.2009.129 [PubMed: 19812543]

Hayasaka S, & Laurienti PJ (2010). Comparison of characteristics between region-and voxel-based network analyses in resting-state fMRI data. Neuroimage, 50(2), 499–508. 10.1016/j.neuroimage.2009.12.051 [PubMed: 20026219]

Ikemoto S. (2007). Dopamine reward circuitry: two projection systems from the ventral midbrain to the nucleus accumbens–olfactory tubercle complex. Brain research reviews, 56(1), 27–78. 10.1016/j.brainresrev.2007.05.004 [PubMed: 17574681]

Knutson B, & Gibbs SE (2007). Linking nucleus accumbens dopamine and blood oxygenation. Psychopharmacology, 191(3), 813–822. 10.1007/s00213-006-0686-7 [PubMed: 17279377]

Kringelbach ML, & Rolls ET (2004). The functional neuroanatomy of the human orbitofrontal cortex: evidence from neuroimaging and neuropsychology. Progress in neurobiology, 72(5), 341–372. 10.1016/j.pneurobio.2004.03.006 [PubMed: 15157726]

Kupchik YM, & Prasad AA (2021). Ventral pallidum cellular and pathway specificity in drug seeking. Neuroscience & Biobehavioral Reviews, 131, 373–386. 10.1016/j.neubiorev.2021.09.007 [PubMed: 34562544]

Lutz K, & Widmer M (2014). What can the monetary incentive delay task tell us about the neural processing of reward and punishment. Neuroscience and Neuroeconomics, 3(3), 33–45. 10.2147/NAN.S38864

Miller BL, Darby AL, Swartz JR, Yener GG, & Mena I (1995). Dietary changes, compulsions and sexual behavior in frontotemporal degeneration. Dementia and Geriatric Cognitive Disorders, 6(4), 195–199. 10.1159/000106946

Morris JC (1993). Current vision and scoring rules the clinical dementia rating (CDR). Neurology, 43(11), 2412–2414. 10.1212/WNL.43.11.2412-a

Pauli WM, Nili AN, & Tyszka JM (2018). A high-resolution probabilistic in vivo atlas of human subcortical brain nuclei. Scientific data, 5(1), 1–13. 10.1038/sdata.2018.63 [PubMed: 30482902]

Perry DC, Datta S, Sturm VE, Wood KA, Zakrzewski J, Seeley WW, & Rosen HJ (2017). Reward deficits in behavioural variant frontotemporal dementia include insensitivity to negative stimuli. Brain, 140(12), 3346–3356. 10.1093/brain/awx259 [PubMed: 29053832]

Perry DC, Sturm VE, Seeley WW, Miller BL, Kramer JH, & Rosen HJ (2014). Anatomical correlates of reward-seeking behaviours in behavioural variant frontotemporal dementia. Brain, 137(6), 1621–1626. 10.1093/brain/awu075 [PubMed: 24740987]

Perry DC, Sturm VE, Wood KA, Miller BL, & Kramer JH (2015). Divergent processing of monetary and social reward in behavioral variant frontotemporal dementia and Alzheimer's disease. Alzheimer disease and associated disorders, 29(2), 161. 10.1097/WAD.0000000000000012 [PubMed: 24164741]

Perry DC, & Kramer JH (2015). Reward processing in neurodegenerative disease. Neurocase, 21(1), 120–133. 10.1080/13554794.2013.873063 [PubMed: 24417286]

Pribiag H, Shin S, Wang EHJ, Sun F, Datta P, Okamoto A, & Lim BK (2021). Ventral pallidum DRD3 potentiates a pallido-habenular circuit driving accumbal dopamine release and cocaine seeking. Neuron, 109(13), 2165–2182. 10.1016/j.neuron.2021.05.002 [PubMed: 34048697]

Radua J, Vieta E, Shinohara R, Kochunov P, Quidé Y, Green MJ, & Pineda-Zapata J (2020). Increased power by harmonizing structural MRI site differences with the ComBat batch adjustment method in ENIGMA. Neuroimage, 218, 116956. 10.1016/j.neuroimage.2020.116956 [PubMed: 32470572]

Ranasinghe KG, Rankin KP, Pressman PS, Perry DC, Lobach IV, Seeley WW, & Miller BL (2016). Distinct subtypes of behavioral variant frontotemporal dementia based on patterns of network degeneration. JAMA neurology, 73(9), 1078–1088. 10.1001/jamaneurol.2016.2016 [PubMed: 27429218]

Rascovsky K, Hodges JR, Knopman D, Mendez MF, Kramer JH, Neuhaus J, & Miller BL (2011). Sensitivity of revised diagnostic criteria for the behavioural variant of frontotemporal dementia. Brain, 134(9), 2456–2477. 10.1093/brain/awr179 [PubMed: 21810890]

Rolls ET (2019). The cingulate cortex and limbic systems for emotion, action, and memory. Brain Structure and Function, 224(9), 3001–3018. 10.1007/s00429-019-01945-2 [PubMed: 31451898]

Rolls ET, Huang CC, Lin CP, Feng J, & Joliot M (2020). Automated anatomical labelling atlas 3. Neuroimage, 206, 116189. 10.1016/j.neuroimage.2019.116189 [PubMed: 31521825]

Rolls ET, Kringelbach ML, & De Araujo IE (2003). Different representations of pleasant and unpleasant odours in the human brain. European Journal of Neuroscience, 18(3), 695–703. 10.1046/j.1460-9568.2003.02779.x [PubMed: 12911766]

Root DH, Melendez RI, Zaborszky L, & Napier TC (2015). The ventral pallidum: subregion-specific functional anatomy and roles in motivated behaviors. Progress in neurobiology, 130, 29–70. 10.1016/j.pneurobio.2015.03.005 [PubMed: 25857550]

Rubinov M, & Sporns O (2010). Complex network measures of brain connectivity: uses and interpretations. Neuroimage, 52(3), 1059–1069. 10.1016/j.neuroimage.2009.10.003 [PubMed: 19819337]

Shackman AJ, Salomons TV, Slagter HA, Fox AS, Winter JJ, & Davidson RJ (2011). The integration of negative affect, pain and cognitive control in the cingulate cortex. Nature Reviews Neuroscience, 12(3), 154–167. 10.1038/nrn2994 [PubMed: 21331082]

Schultz W. (2010). Dopamine signals for reward value and risk: basic and recent data. Behavioral and brain functions, 6(1), 1–9. 10.1186/1744-9081-6-24 [PubMed: 20047681]

Shinagawa S, Babu A, Sturm V, Shany-Ur T, Toofanian Ross P, Zackey D, & Rankin KP (2015). Neural basis of motivational approach and withdrawal behaviors in neurodegenerative disease. Brain and behavior, 5(9), e00350. 10.1002/brb3.350 [PubMed: 26442751]

Silva MME, Viveiros CP, Kotsifas NJE, Duarte A, Dib E, Mercer PBS, Pessoa RR, Witt MCZ (2019) Olfactory impairment in frontotemporal dementia: A systematic review and meta-analysis. Dementia & neuropsychologia, 13(2):154–161. 10.1590/1980-57642018dn13-020003 [PubMed: 31285789]

Silvetti M, Alexander W, Verguts T, & Brown JW (2014). From conflict management to reward-based decision making: actors and critics in primate medial frontal cortex. Neuroscience & Biobehavioral Reviews, 46, 44–57. 10.1016/j.neubiorev.2013.11.003 [PubMed: 24239852]

Smith KS, & Berridge KC (2005). The ventral pallidum and hedonic reward: neurochemical maps of sucrose "liking" and food intake. Journal of neuroscience, 25(38), 8637–8649. 10.1523/JNEUROSCI.1902-05.2005 [PubMed: 16177031]

Smith KS, Tindell AJ, Aldridge JW, & Berridge KC (2009). Ventral pallidum roles in reward and motivation. Behavioural brain research, 196(2), 155–167. 10.1016/j.bbr.2008.09.038 [PubMed: 18955088]

Sporns O. (2022). Structure and function of complex brain networks. Dialogues in clinical neuroscience. 10.31887/DCNS.2013.15.3/osporns

Sturm VE, Yokoyama JS, Eckart JA, Zakrzewski J, Rosen HJ, Miller BL, & Levenson RW (2015). Damage to left frontal regulatory circuits produces greater positive emotional reactivity in frontotemporal dementia. Cortex, 64, 55–67. 10.1016/j.cortex.2014.10.002 [PubMed: 25461707]

Thomopoulos SI, Nir TM, Villalon-Reina JE, Zavaliangos-Petropulu A, Maiti P, Zheng H, .& Thompson PM (2021). Diffusion MRI metrics and their relation to dementia severity: effects of harmonization approaches. In 17th International Symposium on Medical Information Processing and Analysis (Vol. 12088, pp. 166–179). SPIE. 10.1117/12.2606337

Tindell AJ, Smith KS, Peciña S, Berridge KC, & Aldridge JW (2006). Ventral pallidum firing codes hedonic reward: when a bad taste turns good. Journal of neurophysiology, 96(5), 2399–2409. 10.1152/jn.00576.2006 [PubMed: 16885520]

Torbati ME, Minhas DS, Ahmad G, O'Connor EE, Muschelli J, Laymon CM, & Tudorascu DL (2021). A multi-scanner neuroimaging data harmonization using RAVEL and ComBat. Neuroimage, 245, 118703. 10.1016/j.neuroimage.2021.118703 [PubMed: 34736996]

Torralva T, Kipps CM, Hodges JR, Clark L, Bekinschtein T, Roca M, & Manes F (2007). The relationship between affective decision-making and theory of mind in the frontal variant of fronto-temporal dementia. Neuropsychologia, 45(2), 342–349. 10.1016/j.neuropsychologia.2006.05.031 [PubMed: 16893555]

Touroutoglou A, Hollenbeck M, Dickerson BC, & Barrett LF (2012). Dissociable large-scale networks anchored in the right anterior insula subserve affective experience and attention. Neuroimage, 60(4), 1947–1958. 10.1016/j.neuroimage.2012.02.012 [PubMed: 22361166]

van Steenbergen H, Band GP, Hommel B, Rombouts SA, & Nieuwenhuis S (2015). Hedonic hotspots regulate cingulate-driven adaptation to cognitive demands. Cerebral Cortex, 25(7), 1746–1756. 10.1093/cercor/bht416 [PubMed: 24451656]

Whitwell JL, Sampson EL, Loy CT, Warren JE, Rossor MN, Fox NC, & Warren JD (2007). VBM signatures of abnormal eating behaviours in frontotemporal lobar degeneration. Neuroimage, 35(1), 207–213. 10.1016/j.neuroimage.2006.12.006 [PubMed: 17240166]

Woolley JD, Gorno-Tempini ML, Seeley WW, Rankin K, Lee SS, Matthews BR, & Miller BL (2007). Binge eating is associated with right orbitofrontal-insular-striatal atrophy in frontotemporal dementia. Neurology, 69(14), 1424–1433. 10.1212/01.wnl.0000277461.06713.2 [PubMed: 17909155]

Xiong A, & Wesson DW (2016). Illustrated review of the ventral striatum's olfactory tubercle. Chemical senses, 41(7), 549–555. 10.1093/chemse/bjw069 [PubMed: 27340137]

Zaehle T, Bauch EM, Hinrichs H, Schmitt FC, Voges J, Heinze HJ, & Bunzeck N (2013). Nucleus accumbens activity dissociates different forms of salience: evidence from human intracranial recordings. Journal of Neuroscience, 33(20), 8764–8771. 10.1523/JNEUROSCI.5276-12.2013 [PubMed: 23678119]

Zamboni G, Huey ED, Krueger F, Nichelli PF, & Grafman J (2008). Apathy and disinhibition in frontotemporal dementia: insights into their neural correlates. Neurology, 71(10), 736–742. 10.1212/01.wnl.0000324920.96835.9 [PubMed: 18765649]

Zhang CH (2010). Nearly unbiased variable selection under minimax concave penalty. The Annals of statistics, 38(2), 894–942. 10.1214/09-AOS729

Zhang L, Flagan TM, Häkkinen S, Chu SA, Brown JA, Lee AJ, & ARTFL/LEFFTDS/ALLFTD Consortia. (2023). Network connectivity alterations across the MAPT mutation clinical spectrum. Annals of neurology, 94(4), 632–646. 10.1002/ana.26738 [PubMed: 37431188]

Zhou J, Greicius MD, Gennatas ED, Growdon ME, Jang JY, Rabinovici GD, & Seeley WW (2010). Divergent network connectivity changes in behavioural variant frontotemporal dementia and Alzheimer's disease. Brain, 133(5), 1352–1367. 10.1093/brain/awq075 [PubMed: 20410145]

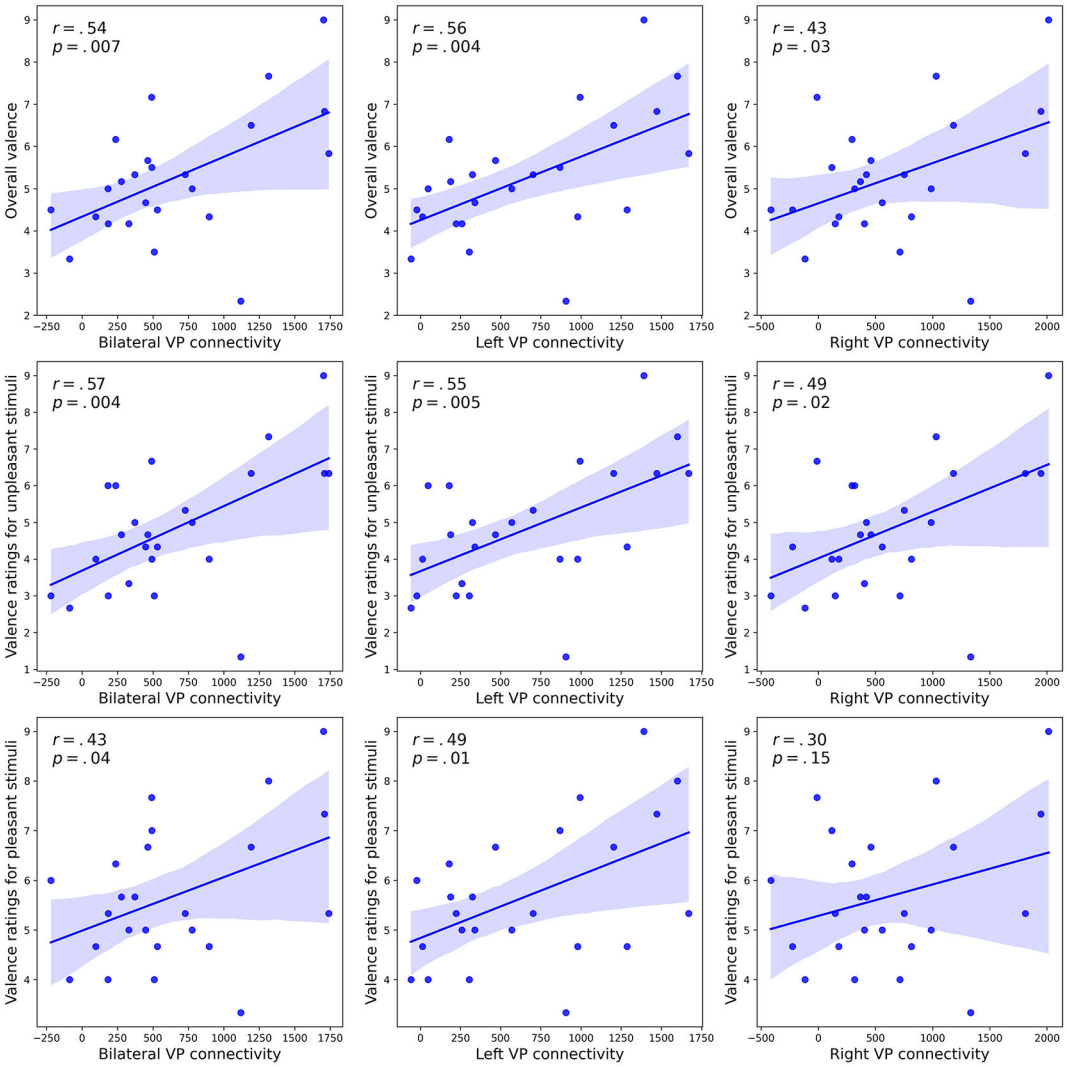

Figure 1.

Correlations between valence and ventral pallidum connectivity. Connectivity represents the sum of correlation between the node and all the other voxels within a mask.

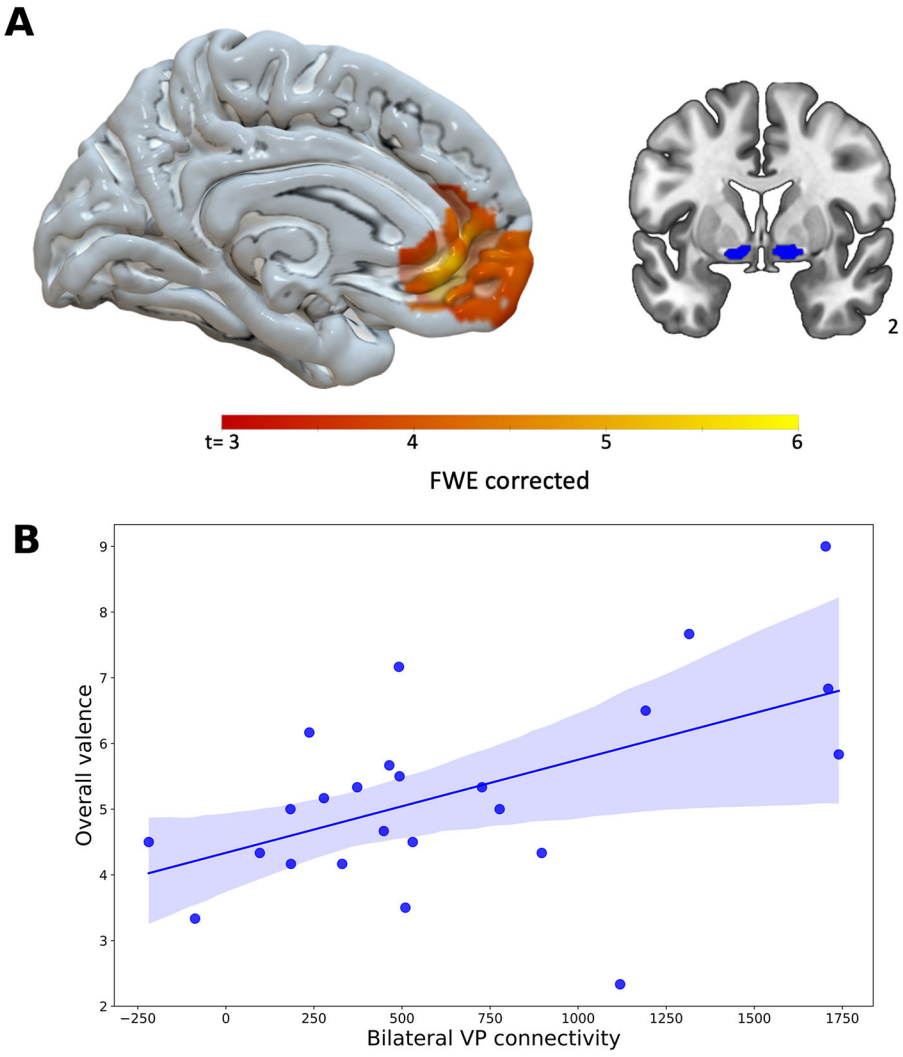

Figure 2.

(A) Seed-based functional connectivity of bilateral ventral pallidum to all other reward regions as a predictor of mean valence ratings ($p < .001$; FWE < .05). Ventral pallidum seed represented in blue. (B) Scatter plot of the relationship between connectivity and the mean valence ratings. VP – ventral pallidum.

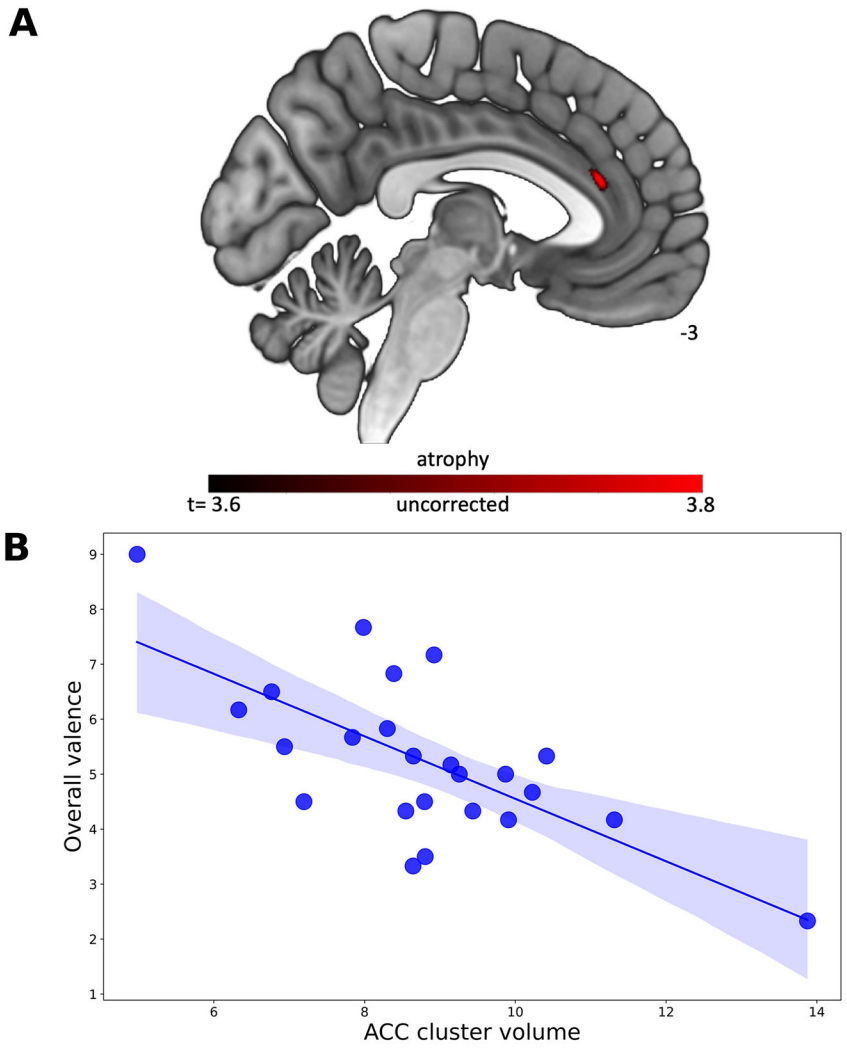

Figure 3.

(A) The relationships of voxel-wise atrophy with valence ratings ($p < .001$, uncorrected). (B) Scatter plot of the relationship between ACC cluster volume (mm^3) and the mean valence ratings. ACC – anterior cingulate cortex.

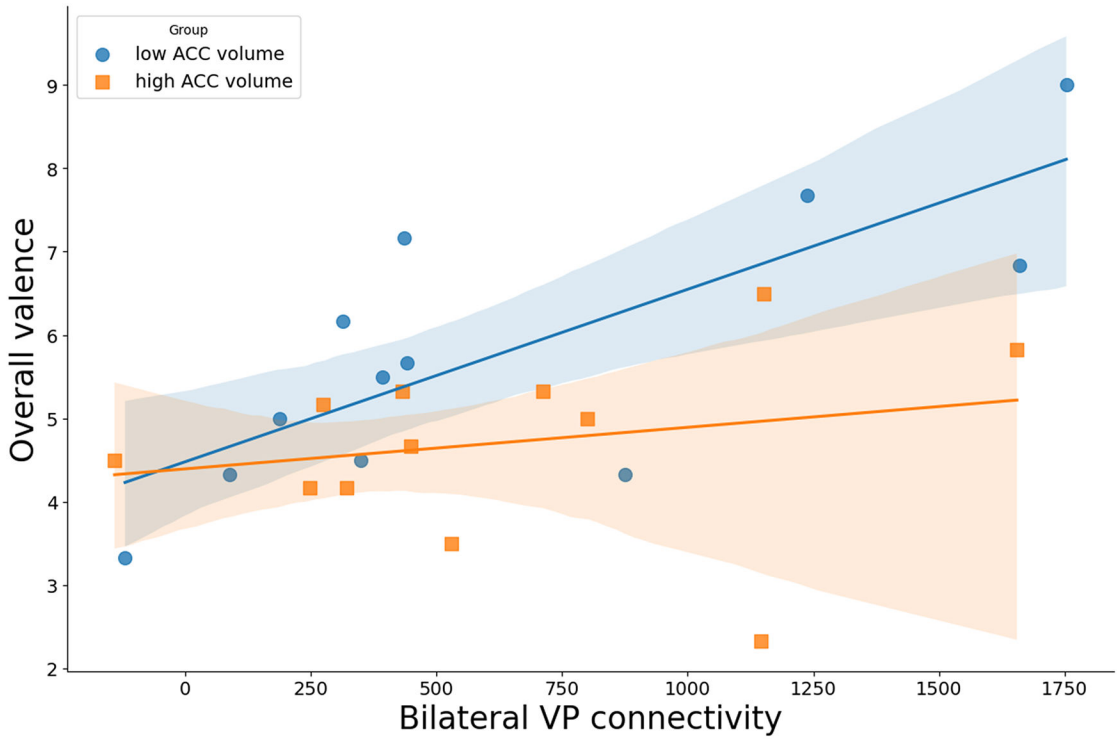

Figure 4.
Interaction between bilateral ventral pallidum functional connectivity and the volume of ACC. ACC – pregenual anterior cingulate cortex, VP – ventral pallidum.